

Explicit periodic solutions in a model of a relay controller with delay and forcing

David A.W. Barton, Bernd Krauskopf, and R. Eddie Wilson

Bristol Centre for Applied Nonlinear Mathematics, Department of Engineering Mathematics, University of Bristol, Queen's Building, Bristol, BS8 1TR, UK

Abstract. In this paper we use a combination of numerical and analytical methods to find and construct solutions of a cameo model of relay control, formulated as a piecewise-constant delay differential equation (DDE). Numerical solutions of a related equation, where the discontinuities of the original DDE are smoothed out, are used to guide the construction of explicit solutions of the original DDE. On the other hand, the construction of explicit solutions provides starting data for numerical continuation of the smoothed equation. The stability of the explicit solutions can also be inferred from the numerical approach.

Submitted to: *Nonlinearity*

1. Introduction

Many physical systems are characterized by non-smooth behaviour. Examples are geared systems [23], where the non-smoothness is due to free-play, and systems involving friction [4], which show slip-stick dynamics. Another class of examples is given by relay control systems. In relay control (also known as bang-bang control) a controller switches between different modes of operation in response to the state of the system [25, 31]. A simple example of such a relay controller is the thermostat switch of a baking oven, which switches the heating element on or off depending on the temperature. In an abstract setting this switching behaviour corresponds to a separation of the phase-space of the system into disjoint regions governed by different dynamics. One speaks of a piecewise smooth dynamical system; see [19, 30, 31] as general references. The non-smooth character of the system may lead to new effects, such as sliding [3] and grazing [22] bifurcations.

We are interested here in the dynamics of relay control systems when there is a fixed time delay τ in the response of the system. There are many possible sources of such a delay, including reaction time delay in a human observer [2], sampling delays [18], actuation delays [16], and communication delays [20]. In many situations the delay is too large to be ignored, so that one is, in fact, dealing with a set of piecewise-smooth delay differential equations.

Delay differential equations (DDEs) are dynamical systems with an infinite dimensional phase-space [14]. This is due to the fact that in the single fixed delay case, a solution history over the delay interval $[-\tau, 0]$ must be specified as the initial condition. The study of delay effects on smooth dynamical systems is thus an active area of research in itself; see [5, 14, 28]. For a recent overview of time delay systems in the context of smooth control we refer to [24].

It is a considerable challenge to understand the possible dynamics and bifurcations in piecewise-smooth delay equations. In this paper we consider a setting in which explicit solutions can be constructed. Specifically, we study a cameo model for a relay controller of an externally forced system with delayed feedback, namely the *non-smooth equation*

$$\frac{dx}{dt} = \text{sign}(f_A(t) - x(t - 1)), \quad (1)$$

where $f_A(t) := Af(t/T)$, and f is the period-1, unbiased square-wave function

$$f(t) = \begin{cases} +1, & 0 \leq t < \frac{1}{2}, \\ -1, & \frac{1}{2} \leq t < 1, \end{cases} \quad (2)$$

with period-1 extension. Thus equation (1) is subject to a periodic forcing, which drives the dynamics. The forcing could be quite general, but here we restrict for definiteness to the square-wave case. The use of square-wave forcing is motivated in the context of relay control by the technique of dithering [15], where a high frequency forcing function is used within a relay controller to stabilise an equilibrium of a nonlinear system. Note that the solutions of the non-smooth equation (1) are piecewise-linear in time, so that it appears possible to construct explicit solutions of (1).

To construct solutions of (1)–(2) we employ analytical construction techniques in parallel with the numerical continuation of solutions [26]. To do this we consider the *smoothed equation*

$$\frac{dx}{dt} = \tanh\left(\frac{f_A(t) - x(t - 1)}{\varepsilon}\right). \quad (3)$$

To obtain a system of smooth autonomous DDEs that approximates the original non-smooth equations (1)–(2), we set $f_A = Ay(\frac{2(1+\delta)}{T}t)$ where $y(t)$ is the solution of

$$\delta \frac{dy}{dt} = -y(t) - (1 + \lambda)y(t - 1) + by^3(t - 1). \quad (4)$$

The DDE (4) is known to have square-wave-like solutions [13] for appropriate choices of the parameters. We found that $\delta = 0.02$, $\lambda = 0.01$, and $b = 0.01$ is a good choice and we use it throughout this paper. Note that ε controls the smoothing of the sign term in the main equation, while δ controls the smoothing of the forcing. Equations (3) and (4) form a system of autonomous DDEs that approximates the original non-smooth problem (1)–(2). With the smoothed equations in this form we are able to use numerical continuation techniques.

Numerical simulation of the initial value problem given by (1)–(2) reveals that the dynamics may be quite complicated. Specifically, one finds three principal classes of solution:

- period- T solutions, where the solution period is equal to the forcing period T ,
- period-4 solutions, where the solution period is four times the delay (i.e., equal to the period of the stable solution of the unforced equation (1)),
- quasi-periodic and more complicated solution types.

In this paper we concentrate on the first two classes, that is, on period- T solutions and on period-4 solutions, because they appear to constitute the ‘backbone’ of the dynamics of the system.

Period- T solutions exist when the forcing amplitude A is large in comparison with the forcing period T . For sufficiently large values of A , the period- T solutions possess two switching points per period, where we define a switching point as the time at which a change in the sign of $f_A(t) - x(t - 1)$ occurs, i.e., a switching point is a local minimum or a local maximum in the solution. This definition applies to both the solutions of the non-smooth equation (1) and to the solutions of smoothed equation (3). As the solutions of (1) are composed of segments that are linear in time, where $dx/dt = \pm 1$, we are able to construct solutions explicitly by considering only the switching points of the solution. The explicit construction and numerical continuation of these period- T solutions is presented in section 2.

Period-4 solutions exist when the forcing amplitude A is small in comparison with the forcing period T . The period-4 solutions have a more complex structure than the period- T solutions; that is, they possess more switching points per period. Consequently their construction is more difficult. Rather than using analytical construction alone, in section 3 we combine the analytical construction of solutions with numerical continuation to prove the existence of branches of period-4 solutions and to investigate their stability. We note that many of the solutions of (1)–(2) have the symmetry

$$x(t + \sigma) = -x(t) \tag{5}$$

where σ is half the period of the solution. We remark that the solutions of (4) possess the symmetry (5) only approximately. Consequently the numerical solutions of the smoothed equations (3)–(4) also possess the symmetry (5) only approximately.

Throughout this paper we use the software package DDE-BIFTOOL [9] to continue numerically solutions of the smoothed equations (3)–(4). DDE-BIFTOOL is a Matlab package that extends to the DDE case much of the functionality of standard continuation packages, such as AUTO [6, 7]. In particular, it enables us to follow periodic orbits while providing stability information (namely, the leading Floquet multipliers).

We finish this introduction by discussing related work. Fridman *et al.* [11, 10] consider a similar model, namely the first order DDE

$$\frac{dx}{dt} = g(x, t) - \text{sign}(x(t - 1)), \quad |g(x, t)| \leq p < 1. \tag{6}$$

In fact, equation (6) can be brought into the form of (1) by the transformation

$$g(x, t) = \frac{df_A}{dt}.$$

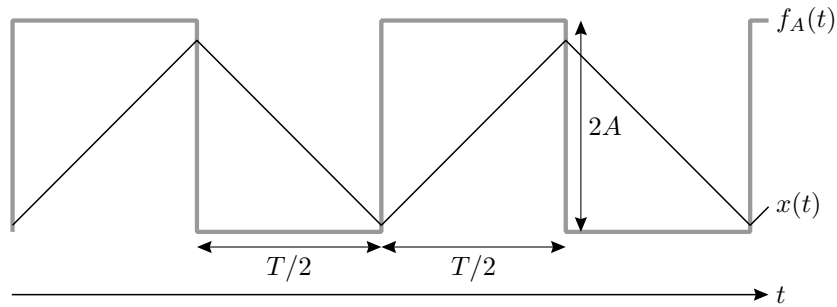


Figure 1. Any period- T solution $x(t)$ of (1), where $f_A(t)$ is unbiased square-wave forcing, possesses translational invariance for a sufficiently large forcing amplitude A .

The assumption that $|g(x, t)| < p \leq 1$ ensures that the sign of the right-hand-side of (6) is determined solely by the value of $x(t - 1)$. This assumption is used in [11, 10] to prove (without construction) the existence and stability of a family of periodic solutions that have the same period as the solutions of the unforced problem. Furthermore, [11, 10] does not encompass forcing functions g that have unbounded or discontinuous derivatives, such as the square-wave forcing considered here. The approach of considering a system for which solutions can be constructed explicitly was also taken in [1, 21]. Norbury and Wilson [21] considered a period- T forced, linear delay model with saturation. For sufficiently large forcing amplitude, they constructed period- T solutions, but due to the more complicated form of the model, sharp existence boundaries were not derived. Bayer and an der Heiden [1] studied a model for delayed relay control in the form of a second order DDE (without forcing). They use analytical techniques to construct explicit solutions and numerical simulation of the initial value problem to investigate the stability of the solutions.

2. Period- T solutions

We now determine the domain of existence in the (T, A) -plane of the period- T solutions that possess two switching points per period; these solutions are typical when the forcing amplitude A is large. Figure 1 shows an example of such a solution. We first consider explicit analytical solutions of the non-smooth equations (1)–(2). Later, smooth solutions of (3)–(4) are considered and the qualitative similarities between the smoothed and non-smooth DDEs are noted. Our principle result is as follows:

Proposition 1 *There exists a period- T solution of the non-smooth equation (1), under the square-wave forcing (2), that possesses two switching points per period, if and only if*

$$A \geq A_{\min}(T) := \begin{cases} |T/4 - r|, & 1/(n + \frac{1}{2}) \leq T \leq 1/n, \\ T/4, & 1/(n + 1) < T < 1/(n + \frac{1}{2}), \end{cases} \quad (7)$$

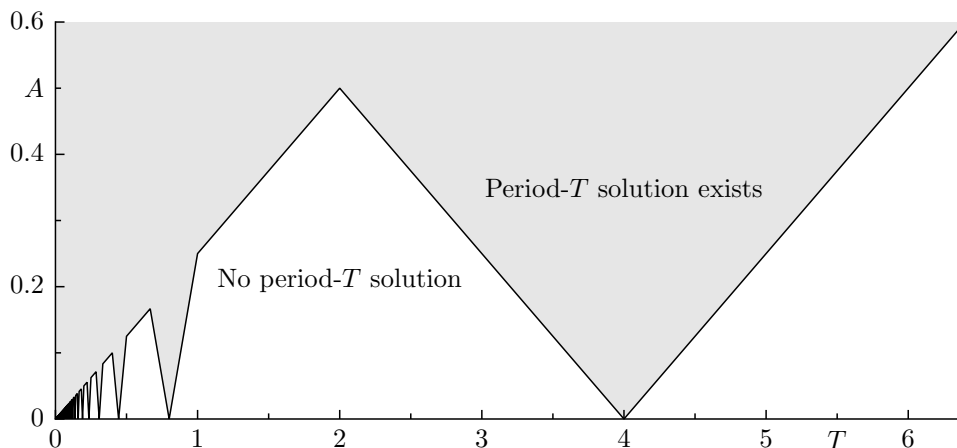


Figure 2. For parameter values in the shaded area of the figure there exists a set of period- T solutions of (1)–(2) that have two switching points per period. The tongue-like grooves are centred on the values of T for which there exists a period- T solution of the unforced equation.

where $n = 0, 1, 2, \dots$, and r is the phase difference between $x(t)$ and $x(t - 1)$ as defined by

$$1 = nT + r.$$

The proof of proposition 1, which involves an explicit construction of solutions of (1)–(2), is technical and is deferred to Appendix A.

Figure 2 plots $A_{\min}(T)$ and thus shows the domain of existence of period- T solutions with two switching points. There are infinitely many ‘grooves’ in the existence boundary given by (7) that are centred on $r = T/4$; i.e., where

$$T = 4/(4n + 1), \quad n = 0, 1, 2, \dots$$

Proposition 1 gives no indication of the stability of the constructed solutions. Consequently we now consider how the constructed period- T solutions of (1)–(2) manifest themselves in the smoothed equations (3)–(4) for small values of ε and we use numerical techniques to determine their stability. We numerically simulate (3)–(4) using Simulink (a Matlab package) with a time-delay block. Simulink employs a fourth order Runge-Kutta method with a fixed time step, which we chose sufficiently small for the rapid changes in the solution gradient to be adequately resolved. The simulations show the existence of period- T solutions possessing two switching points per period. These solutions exist and are stable for all values of the forcing period T when the forcing amplitude A is sufficiently large (i.e., $A > T/4$). However, for $T/4 \geq A \geq A_{\min}(T)$, i.e., within the grooves of the existence boundary, the period- T solutions cannot be found by simulation of (3)–(4); this implies that either the solutions do not exist or they are unstable. Hence we require more sophisticated numerical techniques to determine the existence of period- T solutions for the smoothed equations (3)–(4).

Numerical continuation software, in this case DDE-BIFTOOL, can be used to continue the stable solutions found by numerical simulation. Continuation allows us to

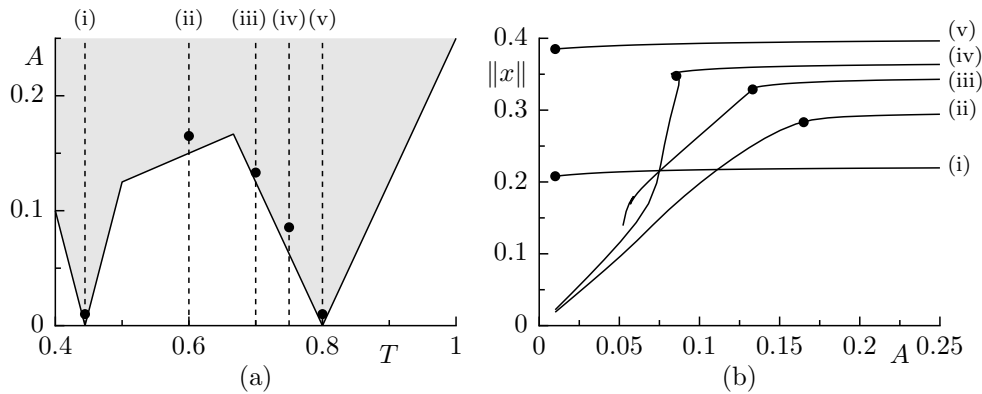


Figure 3. Panel (a) shows a magnified region of the (T, A) -plane of (1)–(2) from figure 2. The dashed lines, labelled (i)–(v), indicate the locations of the five one-parameter continuations of the smoothed equations (3)–(4), shown in panel (b). The continuations show that the solution norm $\|x\|$ remains relatively constant until the value of A comes close to the boundary of existence shown in panel (a). The dots indicate the value of A at which the period- T solution with two switching points deforms into a more complex period- T solution. This is assumed to be when $\|x\|$ reaches 95% of its start value.

trace out a branch of periodic solutions, even though the branch may become unstable at some point. To visualise the solution branches obtained with DDE-BIFTOOL we use throughout the (pseudo-)norm

$$\|x\| := \max x(t) - \min x(t) \quad (8)$$

plotted against the forcing amplitude A .

Figure 3 shows several one-parameter continuations in A for different values of T . Each continuation was started from a stable period- T solution found by simulation of (3)–(4). For $A \geq A_{\min}$ the norm of the explicitly constructed period- T solutions of (1)–(2) remains constant as A is varied. Similarly for $A \geq A_{\min}$ the norm of the smooth period- T solutions of (3)–(4) remains approximately constant. In figure 3 we note with dots the value of A at which the smooth period- T solution with two switching points deforms continuously into a more complex period- T solution. This point is assumed to be when $\|x\|$ reaches 95% of its peak value. The results of the continuation agrees well with the analytic results obtained for the non-smooth equation (1)–(2). The numerical investigation of these solutions shows that both the non-smooth and the smoothed equations possess solutions that, for the same parameter values, are close to each other. This strongly suggests that there also exist period-4 solutions of both equations that are close to each other, and so we can construct explicit solutions of (1)–(2) from the numerical solutions of (3)–(4).

3. Period-4 solutions

When the forcing amplitude A is large, there exists a period- T solution of the non-smooth equations (1)–(2), as is stated by proposition 1. As the value of A is decreased,

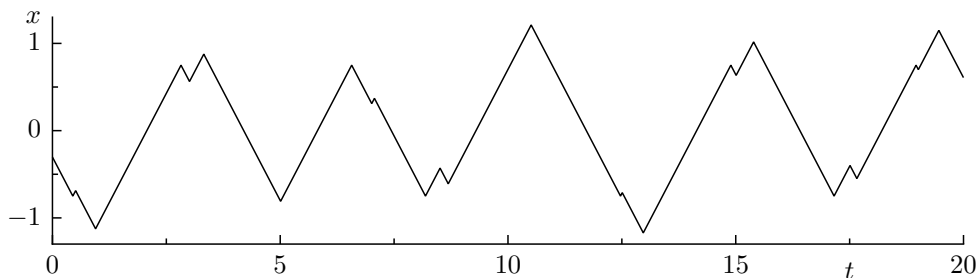


Figure 4. A complex, possibly quasi-periodic solution of the non-smooth equation for $A = 0.24$ and $T = 1$.

this period- T solution ceases to exist at $A = A_{\min}(T)$. From Fridman *et al.* [11] we know that when $A = 0$ (i.e., there is no forcing) the stable solution of (1) has a period of 4. The question we now pose is: what are the intermediate solutions between the period- T solutions at $A = A_{\min}(T)$ and the period-4 solutions at $A = 0$? Numerical simulations of the smoothed equations (3)–(4) show that when the period- T solution loses stability we typically see a transition directly to a period-4 solution or a transition to a quasi-periodic solution and then to more complex solutions. Figure 4 shows a simulation of a complex, possibly quasi-periodic solution.

In this section we find branches of period-4 solutions using a combination of numerical continuation applied to (3)–(4) and the construction of explicit solutions of (1)–(2). DDE-BIFTOOL is used to continue numerically the period-4 solutions of (3)–(4) found by simulation; this gives a branch of period-4 solutions. Solutions on the branch are then constructed explicitly in the limit $\varepsilon \rightarrow 0$, i.e., as a solution of the non-smooth equations (1)–(2).

The explicit construction reveals the existence of additional period-4 solutions that were not found by numerical continuation of the original solution. These additional explicit solutions are then used as starting data for further numerical continuation of (3)–(4), using a small value of the smoothing parameter ε . The numerical continuation leads to the discovery of an additional unstable branch of solutions. Additionally we infer the stability of the non-smooth solutions from the numerical results. Without this combination of numerical and analytical techniques this additional branch would not have been found.

The explicit period-4 solutions of (1)–(2) possess the symmetry (5); the smooth solutions of equation (3)–(4) possess this type of symmetry only approximately, i.e., $x(t) \approx x(-t + 2)$. However, by decreasing the value of δ we are able to get arbitrarily close to this symmetry. The bifurcation diagram of (1)–(2) shows the existence of symmetry breaking bifurcations. These symmetry breaking bifurcations are unfolded by the slight asymmetry of the smoothed equations giving two disconnected branches.

Throughout this most of this section we fix $\varepsilon = 0.01$. This value presents a good compromise: it provides sufficient smoothing to allow the continuation of solutions while retaining solutions that are close to the non-smooth solutions of (1)–(2). In the final

subsection we consider the effects of varying ε . For values of $\varepsilon > 0.3$ there are significant structural changes to the branches of the period-4 solutions. However, for smaller values of ε there is remarkably little change in the overall structure of the branches.

3.1. Continuation of period-4 solutions

Numerical simulation of the smoothed equations (3)–(4) shows the existence of period-4 solutions possessing two switching points per period; see for example the solution shown in figure 5(b). These period-4 solutions co-exist with the period- T solutions described in section 2.

Period-4 solutions exist for small values of A , centred around vertical lines in the (T, A) plane that pass through the base of the grooves shown in figure 2. The previous construction of period- T solutions in section 2 gives the value of T at the base of the grooves as $T = 4/(1 + 4n)$ where $n = 1, 2, \dots$. Lines (i) and (v) in figure 3(a) are examples of such vertical lines for $T = 4/9$ and $T = 4/5$ respectively. All subsequent numerical continuation is performed along line (i), i.e., A is varied while we fix $T = 4/9$. One of the results of this section is that from this fixed value of T we can deduce the qualitative behaviour of all the other branches of period-4 solutions for $T = 4/(1 + 4n)$.

The period-4 solutions appear to possess the symmetry (5). For the panels (b) and (d) of figure 5 this corresponds to a 180° rotation about the centre of each panel. However the solutions, on close inspection, are slightly asymmetric although this is not easily seen from the figures shown. This slight asymmetry in the solution is caused by an asymmetry in the forcing function f , as was discussed above.

DDE-BIFTOOL was used to continue numerically a solution found by simulation; this solution is shown in figure 5(b). Continuation in the forcing amplitude A gives a branch of period-4 solutions labelled B_I in figure 5(a). The existence of this branch verifies that the simulated solutions are true periodic solutions of (3)–(4) rather than long term transients.

We now discuss in detail the branch B_I . For small values of A there exists a single stable solution, which possesses two switching points per period and appears to be almost symmetric as previously mentioned. Along the branch for $0 < A < 0.30$ the solutions alter very little, so that the norm $\|x\|$ remains nearly constant in this range of A .

At $A \approx 0.30$ a saddle-node (or fold) bifurcation occurs and the solution loses its stability. Immediately after this saddle-node bifurcation, along the bifurcating unstable branch segment, additional switching points emerge in the solution close to the existing switching points. These additional switching points make the solutions very clearly asymmetric, as is illustrated by figure 5(c). A second saddle-node bifurcation occurs on the branch at $A \approx 0.22$ and the solution regains its stability. At this point the solution appears to be almost symmetrical once again; figure 5(d) shows the solution after the second saddle-node bifurcation, in the second stable region. The two saddle-node bifurcations give rise to a hysteresis loop due to the region of bistability for the

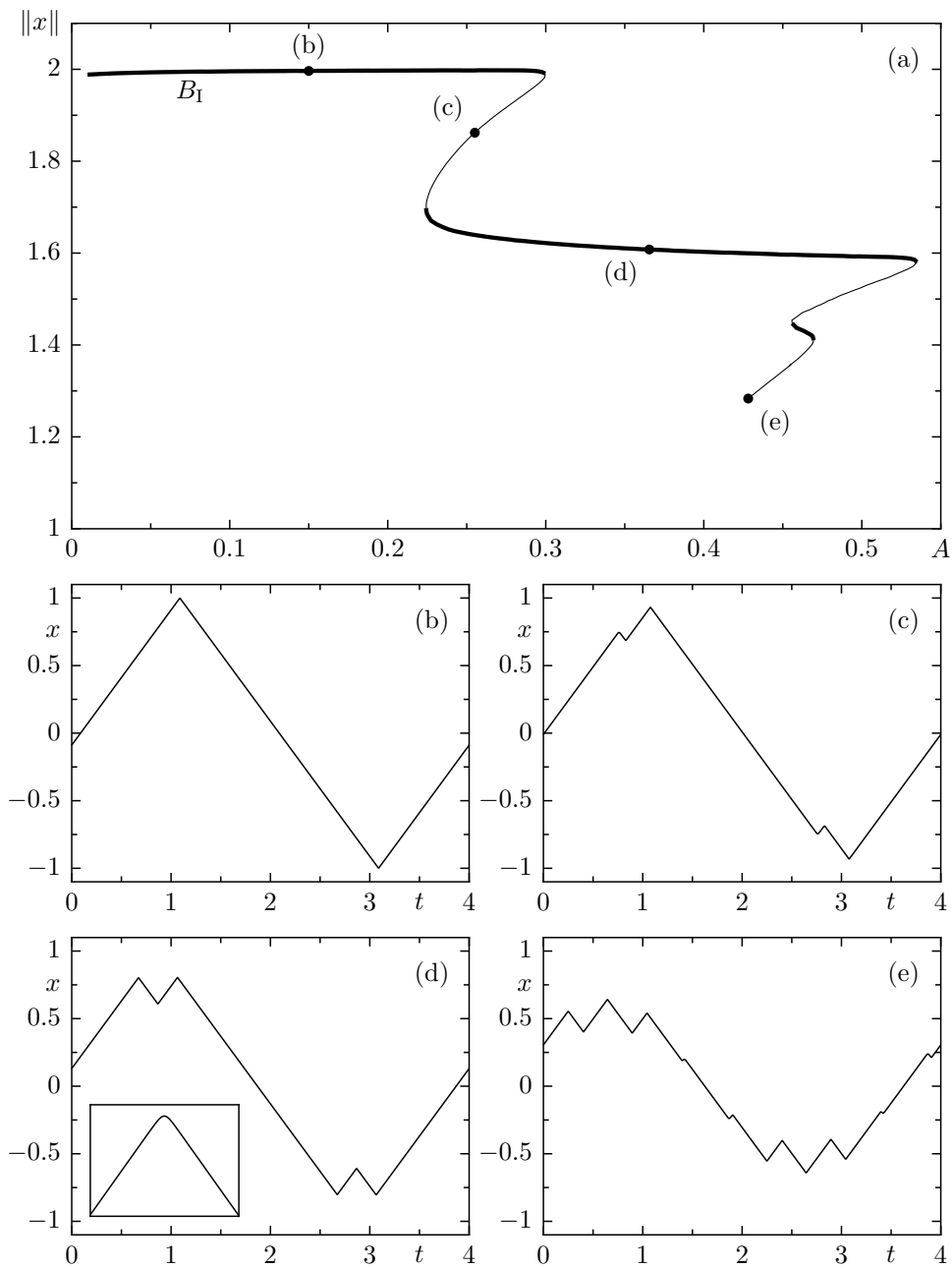


Figure 5. Panel (a) shows branch B_I , a branch of period-4 solutions of the smoothed equations (3)–(4) for $T = 4/9$. The branch was continued from the stable solution, shown in panel (b), that was found by numerical simulation. The bold curves in panel (a) denote stable solutions. Panels (b)–(e) show examples of solutions of (3)–(4) along the branch. These solutions appear non-smooth, however they are completely smooth; solutions found using this value of ε give a good approximation to the non-smooth equation. The inset in panel (d) is an enlargement of the second peak.

range $0.22 < A < 0.30$.

The norm of the solution in the second stable region lies in the range $1.6 < \|x\| < 1.7$; in this second stable region there is greater variation in the value of $\|x\|$ than for the first stable region. Before the first saddle-node bifurcation at $A \approx 0.30$, the value of $x(t)$ at each of the switching points of the solution was much greater than the value of $f_A(t)$, consequently small changes of A have little affect on the solution. In other words, the right-hand side of (3)–(4), $\tanh((f_A(t) - x(t - 1))/\varepsilon)$, remains close to either $+1$ or -1 . In the second stable region, the value of $x(t)$ at the switching points of the solution is closer to the value of A . Consequently small changes in A produce a larger affect on the right-hand side of (3)–(4).

A further saddle-node bifurcation occurs at $A \approx 0.53$, and once again additional switching points emerge making the solutions clearly asymmetric. The solutions become almost symmetric again at a saddle-node bifurcation at $A \approx 0.46$. Although there is a small region of bistability, there is no second hysteresis loop because the branch loses its stability again almost immediately at $A \approx 0.47$.

After this final saddle-node bifurcation the dynamics become even more complex, due to the interactions of the switching points and the forcing function. Figure 5(e) shows a solution on the branch after the final saddle-node bifurcation. As the branch is continued further, it remains unstable and more switching points are formed in the solutions. The increased complexity of the solutions eventually causes convergence problems in the continuation. These problems can be alleviated by increasing the number of mesh points used to represent the solution. However, the number of mesh points soon becomes intractably large.

3.2. *Explicit construction of period-4 solutions*

As we have just demonstrated, numerical continuation of the smoothed equations (3)–(4) for small values of ε shows the existence of a single branch of period-4 solutions. We now show that period-4 solutions also exist for the non-smooth equations (1)–(2).

Proposition 2 *For $T = 4/(1+2n)$, where $n = 1, 2, \dots$, equations (1)–(2) possesses two branches of symmetric period-4 solutions and an even number of branches of asymmetric solutions. The asymmetric branches connect the two branches of symmetric solutions.*

Outline of proof. The numerical period-4 solutions of (3) possess two zeroes per period, such that

$$x(t_0 + 2k) = 0, \quad \text{for } k \in \mathbb{Z}, \tag{9}$$

where t_0 is the location of an arbitrary zero. Also, the forcing period T of those solutions found by numerical simulation is restricted to $T = 4/(1 + 2n)$, for $n = 1, 2, \dots$; for these values of T the forcing function has the property

$$f_A(t + 2) = -f_A(t), \tag{10}$$

for all t . We now determine the requirements placed on the sign changes of $f_A(t) - x(t-1)$ by (9). Integrating (1) gives

$$x(t_0 + 2) = x(t_0) + \int_{t_0}^{t_0+2} \text{sign}(f_A(t) - x(t-1))dt.$$

Combining this with (9) gives

$$\int_{t_0}^{t_0+2} \text{sign}(f_A(t) - x(t-1))dt = 0. \quad (11)$$

Equation (11) states that between any two consecutive zeros in x , the amount of time for which $f_A(t) > x(t-1)$ must equal the amount of time for which $f_A(t) < x(t-1)$.

We now outline the steps to construct the period-4 solutions of (1)–(2); full details are given in Appendix B.

- (i) Set $x(t) = t - t_0$, for $t \in [t_0 - \frac{1}{2}, t_0 + \frac{1}{2}]$.
- (ii) Determine the values of t_0 and A such that (11) is satisfied, assuming that $x(t) < A$ for $t \in [t_0 - 1, t_0 - \frac{1}{2}]$ and that $x(t) > A$ for $t \in [t_0 + \frac{1}{2}, t_0 + 1]$.
- (iii) Extend the solution using the method of steps for $t \in [t_0 + \frac{1}{2}, t_0 + \frac{3}{2}]$ (the method of steps maps an interval of the solution forward in time to extend the existing solution; see [14, Chapter 1]).
- (iv) Determine the values of t_0 and A such that $x(t) > A$ for $t \in [t_0 + \frac{1}{2}, t_0 + \frac{3}{2}]$.

The solution resulting from these steps, for different parameter values, are shown in the left column of figure 6. The right column of figure 6 shows $x(t-1)$ and $f_A(t)$, the intersections of which correspond to the switching points of the solutions in the left column. Since $x(t) > A$ for $t \in [t_0 + \frac{1}{2}, t_0 + \frac{3}{2}]$, we can extend the solution further by the method of steps to produce a linear segment of solution with a derivative of -1 . Also, there is a zero in x at $t = t_0 + 2$ because A and t_0 have been chosen to satisfy (11). Consequently, $x(t) = -(t - t_0 - 2) = -x(t-2)$ for $t \in [t_0 + \frac{3}{2}, t_0 + \frac{5}{2}]$. When combined with (10), this symmetry ensures that the solution will be periodic with period 4 when extended a further time unit by the method of steps.

This method of solution construction requires that $A < \frac{1}{2}$; for $A \geq \frac{1}{2}$ the validity of the assumptions in step (ii) is in doubt. However, it turns out that for all the solutions constructed here, $A < \frac{1}{2}$ for all values of T , except for $T = \frac{4}{3}$ (i.e., for $n = 1$). \square

Figure 7(a) illustrates the four solution branches when $T = 4/9$ constructed in proposition 2. The two symmetric branches B_A and B_B are shown as solid lines, and the two asymmetric branches B_C and B_D are shown as dashed lines. The two symmetric branches, B_A and B_B , do not intersect; the intersections seen in the figure are due to our choice of norm $\|x\|$; the solutions at this point are dissimilar, they each contain different numbers of switching points.

The solutions on the branches B_C and B_D are related by the symmetry $x_1(t) = -x_2(-t)$, where x_1 and x_2 are solutions on the respective branches for the same value of t_0 , the norm (8) does not distinguish between them so that they appear on top of

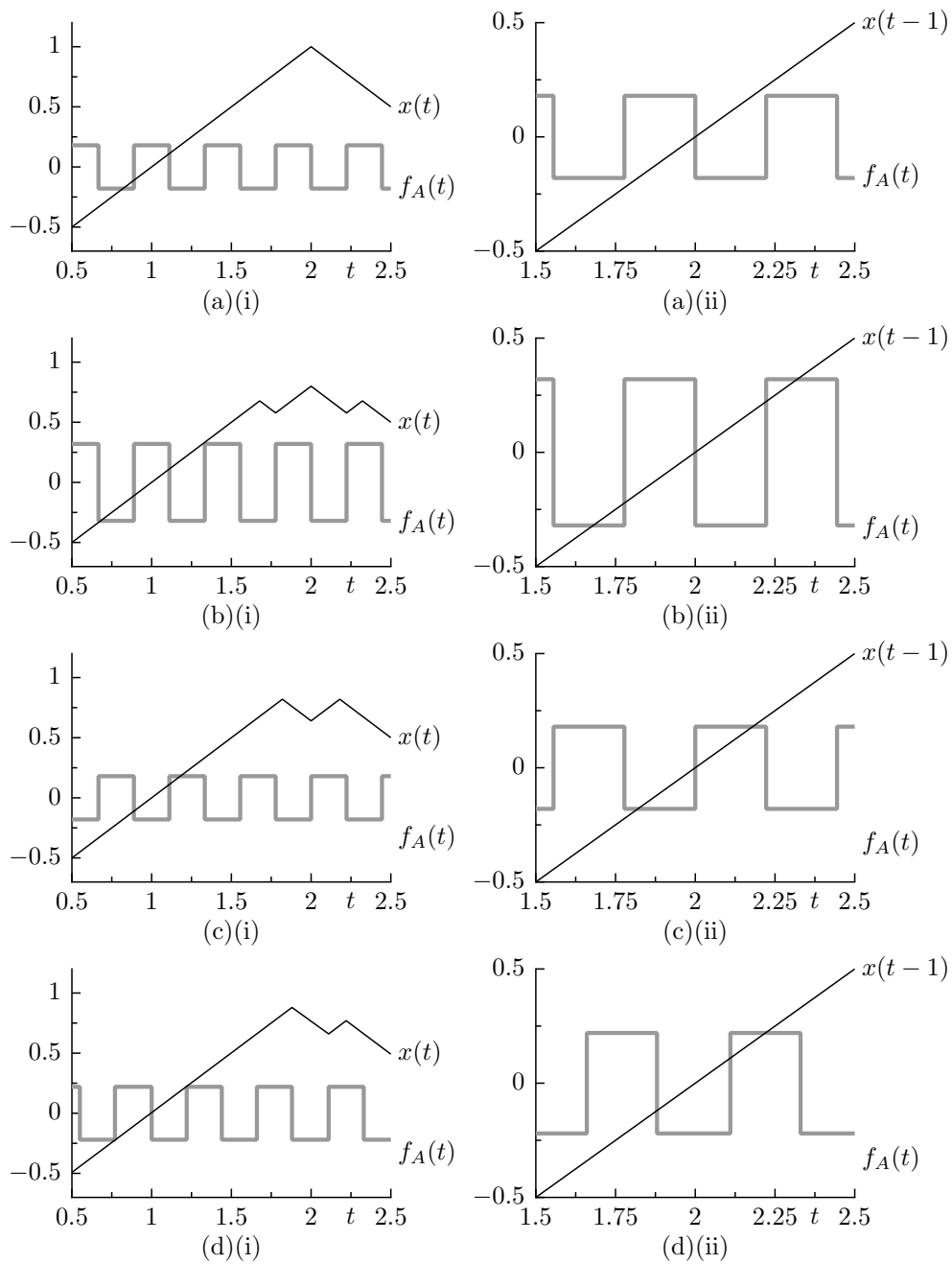


Figure 6. The construction of a period-4 solution of (1)–(2). When the forcing amplitude A is sufficiently small there exist only two switching points during each period, as shown in panel (a)(i). As A is increased, additional switching points are created at $T = 2 \pm T/2$ as shown in panel (b)(i). Panels (c)(i) and (d)(i) show other period-4 solutions that are found by phase shifting the solution in (a)(i) relative to the forcing. Panels (a)(ii), (b)(ii), (c)(ii), and (d)(ii), are magnified regions of panels (a)(i), (b)(i), (c)(i), and (d)(i), respectively, showing intersections of $x(t-1)$ and $f_A(t)$ that cause the creation of switching points in the solution.

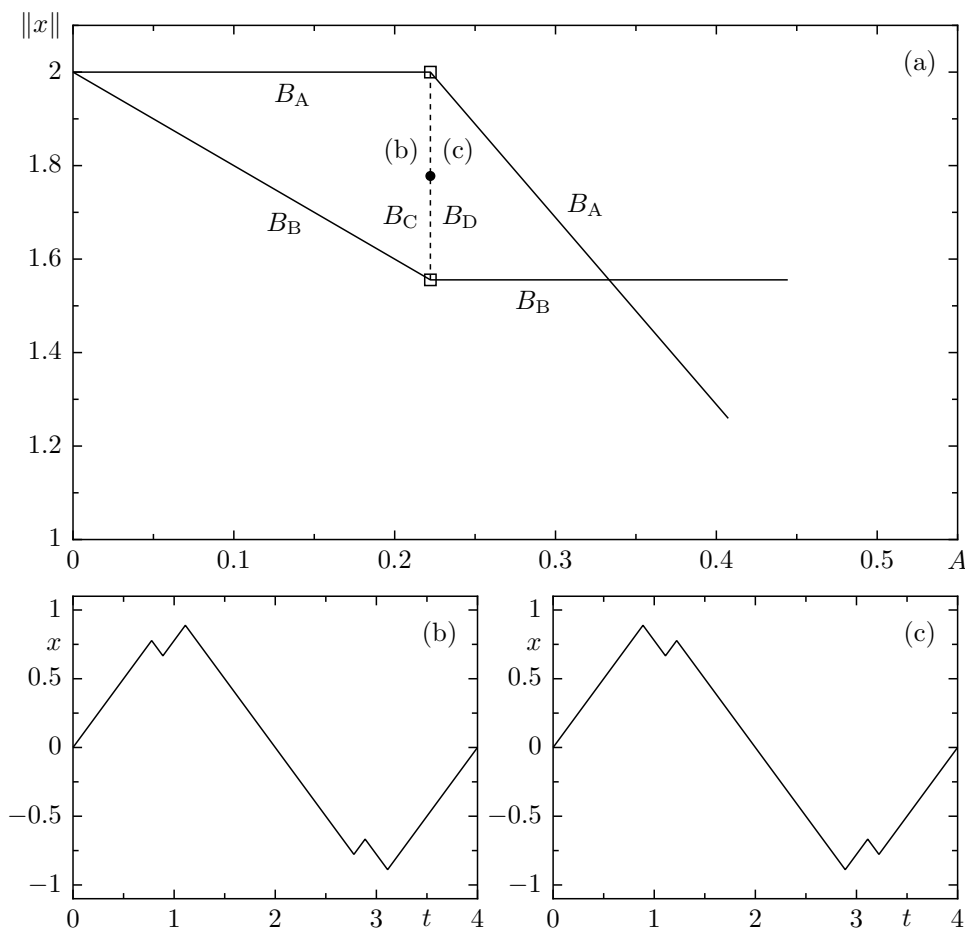


Figure 7. The analytically constructed branches of period-4 solutions of the non-smooth equations (1)–(2) for $T = 4/9$, where the parameter varied is A . Branches B_A and B_B denoted by solid lines contain solutions that possess the exact symmetry (5), and the dashed line denotes the two asymmetric branches B_C and B_D bifurcating from the symmetric branches in a symmetry breaking bifurcation. The solutions in the two asymmetric branches are symmetric counterparts of each other. Consequently, the two branches are plotted on top of each other when using this norm. Panels (b) and (c) show examples of two symmetric counterparts.

each other in figure 7(a). An example of two such solutions that have the same norm is shown in figure 7(b)–(c). Where these asymmetric branches intersect the symmetric branches, the solutions on either branch are identical. This suggests the presence of two symmetry breaking bifurcations as marked by open squares at $A = 0.22$ in figure 7.

At the end of branches B_A and B_B shown in figure 7, the assumption in step (ii) of proposition 1 fails. At this point there is a fold in each of the branches. It is possible to construct explicit solutions to continue the branches B_A and B_B , but this becomes much more involved due to the extra switching points.

We now consider the effect of changing the forcing period T , as well as the forcing amplitude A . As the value of T decreases, additional ‘twists’ of the two symmetric branches will occur, where the value of the norm on each branch is identical for

a particular value of A but the solutions on each branch differ. This leads to an intertwining of the two branches. As the number of twists increases, so will the number of branches of asymmetric solutions and symmetry breaking bifurcations.

3.3. Numerical continuation of analytically constructed solutions

Proposition 2 ensures the existence of two continuous branches of symmetric period-4 solutions of (1)–(2). However in section 3.1 this was not observed in the continuation of solutions of (3)–(4). Since numerical continuation of solutions found by simulation has not revealed the existence of these solutions, this suggests that the branch containing these solutions is entirely unstable. The analytically constructed solutions of (1)–(2) can be used as initial data for the numerical continuation of (3)–(4), so that the second branch of (3)–(4) can also be found.

We use the solution shown in figure 6(c) as initial data for continuation. This reveals a new branch B_{II} of solutions that are all unstable as predicted. The new branch B_{II} is shown along with the branch B_{I} in figure 8. This new branch of solutions “intertwines” with the existing branch. At the intersections of the two branches, the solutions on the respective branches are different. This is again due to the choice of norm used (8).

Comparing figure 7(a) with figure 8(a) we see qualitative differences between the branches of period-4 solutions. Branch B_{I} is composed of a segment of branch B_{A} , branch B_{C} , and a segment of branch B_{B} . Likewise, branch B_{II} is composed of a segment of branch B_{B} , branch B_{D} , and a segment of branch B_{A} . However, for each of the solutions of the smoothed equations (3)–(4) there exists a nearby solution of the non-smooth equations (1)–(2). There are two principle differences between the branches of smooth solutions and the branches of non-smooth, both caused by the smoothing of the forcing. These differences are:

- Branches B_{I} and B_{II} do not have solutions in common, whereas branches B_{A} , B_{B} , B_{C} , and B_{D} intersect at two symmetry breaking bifurcations.
- Branches B_{C} and B_{D} of figure 7(a) are vertical, whereas the equivalent segments of branches B_{I} and B_{II} are slanted.

Considering the first difference, both branches B_{I} and B_{II} of the smoothed equations (3)–(4) contain regions where the solutions are almost symmetric in the sense of (5). Also, for each of the solutions x_1 of B_{I} that is clearly asymmetric (e.g., figure 5(c)), there exists a nearby solution x_2 of B_{II} such that $x_1(t) \approx -x_2(-t)$. This is the symmetry seen between the asymmetric branches of (1)–(2). All these ‘almost’ symmetries in the solutions of (3)–(4) suggest that there has been an unfolding of the symmetry breaking bifurcations [29, Chapter 3] that are present in the analytical construction. The slight asymmetry of the forcing given by (4) also implies that symmetry breaking bifurcations are unfolded.

The unfolding of the symmetry breaking bifurcation separates the two branches B_{C} and B_{D} ; they no longer lie on top of each other in the $(A, \|x\|)$ -plane. Also, the symmetric branches, B_{A} and B_{B} , and asymmetric branches, B_{C} and B_{D} , are split at the

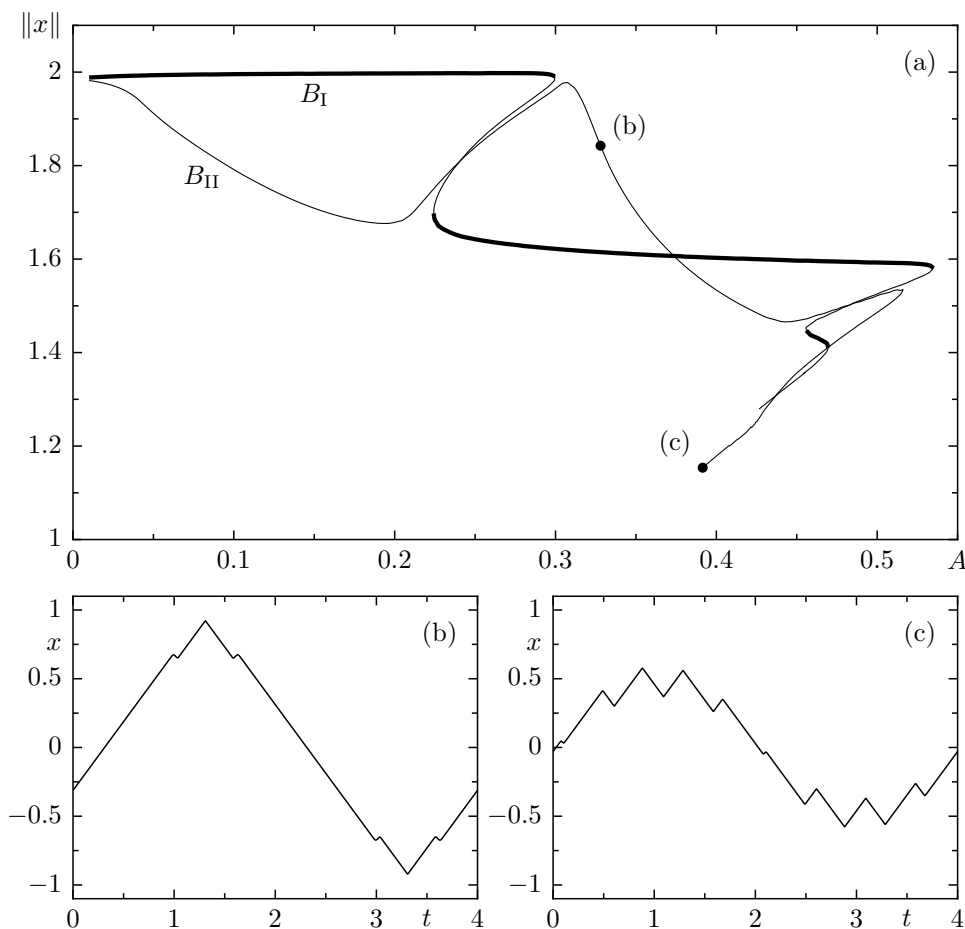


Figure 8. Panel (a) shows both branches B_I and B_{II} of period-4 solutions of the smoothed equations (3)–(4) for $T = 4/9$ where the continuation parameter is A ; c.f., figure 5. Bold lines denote stable solutions; the intersections of the branches are due to the projection used. Panels (b) and (c) show the continued solutions of (3)–(4).

former location of the symmetry breaking bifurcation, producing the two disconnected branches B_I and B_{II} that have regions where the solutions are almost symmetric.

The second difference between figures 7 and 8 is also caused by the smoothing of the forcing function. Consider figure 6(a)(ii); the symmetry breaking bifurcation of branch B_A in figure 7 occurs when A is increased further, causing additional intersections of $x(t - 1)$ and $f_A(t)$. If the forcing function f_A is smoothed, the additional intersections occur at a higher value of A . However the smoothing of the forcing does not significantly effect the location of the symmetry breaking bifurcation of branch B_B . Thus the asymmetric sections of B_I and B_{II} become slanted.

The analytically constructed solutions of (1)–(2) provide us with a great deal of information about the solutions of the smoothed equations (3)–(4). This information leads us to conjecture that decreasing the value of T will lead to an increased number of “twists” in the branches of period-4 solutions, where the norms of the two branches are identical while the solutions on each branch are not. We also conjecture that all

branches that lie approximately horizontal in the $(A, \|x\|)$ -plane are stable and have the symmetry (5). This is indeed confirmed by numerical continuation for smaller values of T .

For the non-smooth equations (1)–(2) we have no stability information for the period-4 solutions, as proving the stability of the solutions analytically would be very tedious. However, from the interplay of the results for both (1)–(2) and (3)–(4), we can infer that the regions of the branches, for which the norm of the solution remains constant, are stable. This shows that studying both equations simultaneously increases our knowledge of each equation individually.

3.4. Varying the smoothing parameter ε

The smoothing parameter ε was assumed to be small. Specifically we used $\varepsilon = 0.01$, which is small enough to give smooth solutions that are nearby to the non-smooth solutions of (1)–(2) and large enough to allow numerical continuation in DDE-BIFTOOL. We now consider the effect of increasing the parameter ε . Panels (a)–(d) of figure 9 show bifurcations diagrams of the period-4 solutions of (3)–(4) for different values of ε . As the smoothing ε is increased there is a noticeable decrease in the solution norm $\|x\|$. The change in the period-4 solutions is shown in figure 9(e) where half a period of a solution is displayed for different values of ε . As shown in figures 9(e), for a fixed value of A , increasing ε creates additional inflections in the solution, although we find no additional switching points. The smooth solutions remain remarkably similar to the analytical solution even for relatively high values of ε .

The effect of changing ε on the branches themselves is that the branches ‘untwist’. For small values of ε there are multiple intersections of the two branches where the solution norms are identical for a particular value of A . As the value of ε is increased the number of intersections of the two branches decreases. The two saddle-node bifurcations in the vicinity of $A \approx 0.24$ come together at a cusp bifurcation.

At $\varepsilon \approx 0.28$ a true intersection of the two branches occurs, that is for a particular value of A the solutions on either branches are identical. This is a singularity in the bifurcation diagram at which the branch structure changes. It occurs at a transition through a saddle, also known as a ‘simple bifurcation’ [12, Chapter 4]. Above this value of ε the two branches separate. For values of A between these two islands, where no period-4 solution exists, numerical simulation shows that the solutions oscillate between two states, one with 4 switching points per period (c.f., figure 8(b)), and one with 6 switching points per period (c.f., figure 5(d)). Increasing ε further decreases the size of the islands and increases the gap between them.

The main effect of increasing the value of the smoothing is that the more complex solutions (i.e., the solutions with many switching points) are gradually lost. However the branches themselves do not change significantly for $\varepsilon < 0.2$. This suggests that the technique of combining numerical methods and analytical construction presented in this paper is quite robust with respect to the smoothing of the original non-smooth DDE. In

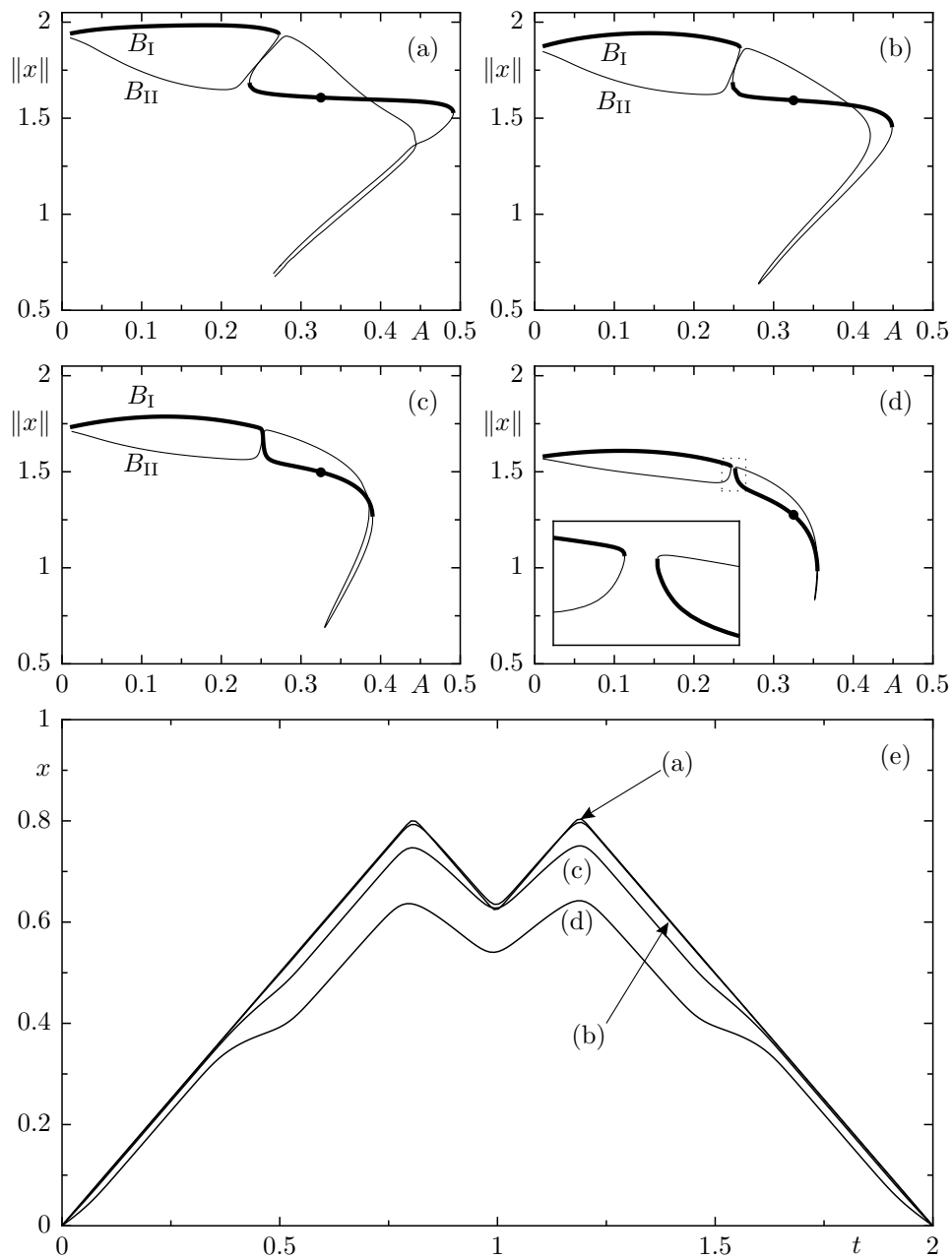


Figure 9. Panels (a)–(d) show the branches of period-4 solutions of the smoothed equation (3) for different values of ε . In panel (a) $\varepsilon = 0.05$; in (b) $\varepsilon = 0.1$; in (c) $\varepsilon = 0.2$; and in (d) $\varepsilon = 0.3$. For larger values of ε (approximately $\varepsilon > 0.28$) the branches separate completely and form two “islands” of solutions. Panel (e) shows individual solutions for a fixed value of A .

fact information can be extracted from the numerical continuations to construct explicit analytical solutions to the non-smooth DDE (1)–(2) even for relatively high values of ε . Thus it seems likely that one may use this technique on more complicated equations that cannot be smoothed as easily as (1).

4. Conclusions

By combining the explicit construction of solutions of a non-smooth equation with the numerical continuation of solutions of a smoothed equation, we are able to gain a complete understanding of period- T and period-4 solutions in a cameo model of a relay control system with delay and forcing. These solutions form a ‘backbone’ of the dynamics and the next step would be to study in detail quasi-periodic and more complicated (possibly chaotic) dynamics and the bifurcations involved in their creation.

A further issue is how the results that we obtained here depend on the forcing function. Work in progress indicates that period- T solutions can be constructed in a similar way for a large class of forcing functions. Furthermore, certain features of the existence diagram (see figure 2) are retained.

The approach taken here could be applied to other piecewise-constant or even piecewise-linear delay differential equations. An example would be the piecewise-smooth DDE

$$\frac{dx}{dt} = x(t) + \text{sign}(f_A(t) - x(t - 1)), \quad (12)$$

which arises naturally from the linearisation of non-linear systems subject to delayed control, such as an inverted pendulum [27].

More generally, the continuation results obtained here are quite robust with respect to the degree of smoothing applied to the non-smooth equation. Therefore, numerical continuation of a suitably smoothed delay equation may also prove useful when one deals with a general piecewise-smooth delay equation, for which explicit solutions cannot be constructed. Presently the use of smoothing in this way has only been applied to piecewise smooth ODEs (for example [8, 17]) and not piecewise-smooth DDEs.

Finally, we mention the longer term goal of reversing the approach taken in this paper. Suppose that one wants to study the dynamics and bifurcations of a DDE arising in some application. A key problem is to find suitable solutions from which to start a bifurcation study, using numerical continuation. The idea would be to approximate the given DDE by a piecewise-smooth DDE, for example, by taking some appropriate limiting case. It might then be possible to construct solutions for the limiting equation, in much the same way as presented here. These solutions could then be continued (in the limiting parameters) to solutions of the original DDE.

Appendix A. Proof of proposition 1

A period- T solution with two switching points consists of two linear segments, each of duration $T/2$. Thus, from (1) a necessary and sufficient condition for the existence of a period- T solution with two switching points and a local minimum at $t = t_0$ is

$$\begin{aligned} f_A(t) - x(t - 1) &> 0, & t_0 < t < t_0 + T/2, \\ f_A(t) - x(t - 1) &< 0, & t_0 + T/2 < t < t_0 + T, \end{aligned} \quad (\text{A.1})$$

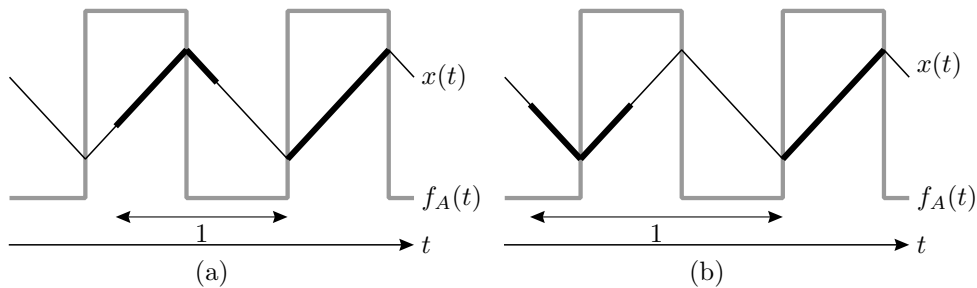


Figure A1. When constructing period- T solutions of (1)–(2), it is necessary to consider one of two possible cases depending on the value of T . Taking half a period of the solution that has a constant positive derivative, the segment of solution one time unit earlier will either contain a local maximum, as in panel (a), or a minimum, as in panel (b).

with period- T extension. Since we seek a solution that has the same period as the forcing, if (A.1) holds for a single period of the solution it will hold for all time. We set

$$x(t) = \begin{cases} t - t_0 - T/4, & t_0 < t < t_0 + T/2, \\ -t + t_0 + 3T/4, & t_0 + T/2 < t < t_0 + T, \end{cases} \quad (\text{A.2})$$

with period T extension, and define the phase difference between $x(t)$ and $x(t - 1)$ as

$$1 = nT + r, \quad n \in \mathbb{Z}, \quad 0 \leq r < T. \quad (\text{A.3})$$

From (A.2) and (A.3) it follows that

$$\begin{aligned} x(t_0 - 1) &= \begin{cases} r - T/4, & 0 \leq r < T/2, \\ 3T/4 - r, & T/2 \leq r < T, \end{cases} \\ x(t_0 + T/2 - 1) &= \begin{cases} T/4 - r, & 0 \leq r < T/2, \\ r - 3T/4, & T/2 \leq r < T. \end{cases} \end{aligned} \quad (\text{A.4})$$

We now determine the values of A , T , and t_0 such that (A.1) holds for the putative solution (A.2).

The value of t_0 is fixed by assuming that the switching points of the solution x are aligned with the discontinuities of the forcing function f so that $f(t_0^+) = A$. The symmetries of the solution, of the forcing function, and of (A.1) ensure that the constraints generated on each half period are equal. Thus, we consider only the first half of the period, $t_0 < t < t_0 + T/2$, for which $f(t) = A$.

For (A.1) to hold on the first half period, the solution must satisfy $x(t - 1) < A$. The maximum value of x is $T/4$, thus the putative solution (A.2) will satisfy (A.1) for $A > T/4$; this is a coarse bound for the existence of a period- T solution with two switching points. To determine the sharp (necessary) bound for the existence of a period- T solution, we now consider how (A.1) can fail as A is decreased.

On a particular range of t the inequality $x(t - 1) < A$ can fail at either a local maximum in the solution, or at the end points of the range. This is illustrated in figure A1. From (A.2) and (A.3), $x(t - 1)$ will possess a local maximum for

$t_0 < t < t_0 + T/2$ if and only if $T/2 < r < T$. The values of the putative solution at the end points of the range are given by (A.4). Thus the sharp (necessary) bound for the existence of a period- T solution with all switching points aligned to the discontinuities in the forcing function is

$$A \geq \begin{cases} |r - T/4|, & 0 \leq r \leq T/2, \\ T/4, & T/2 < r < T. \end{cases} \quad (\text{A.5})$$

We now consider the existence of solutions that fail to satisfy our original assumption on the alignment of the switching points of the solution. Thus, we now assume that the forcing function is continuous at the switching points of the solution $x(t)$. From (A.1) we now have

$$\begin{aligned} f_A(t_0) - x(t_0 - 1) &= 0, & (\text{A.6}) \\ \frac{d}{dt}[f_A(t) - x(t - 1)]|_{t=t_0} &> 0, \\ f_A(t_0 + T/2) - x(t_0 + T/2 - 1) &= 0, \\ \frac{d}{dt}[f_A(t) - x(t - 1)]|_{t=t_0} &< 0. \end{aligned}$$

Since at $t = t_0$ there is a minimum in the solution, from (A.3) we have

$$\begin{aligned} \frac{d}{dt}[x(t - 1)]|_{t=t_0} &= -1, & 0 < r < T/2, \\ \frac{d}{dt}[x(t - 1)]|_{t=t_0} &= +1, & T/2 < r < T. \end{aligned}$$

Consequently, a solution can exist only for $0 < r < T/2$. Substituting (A.4) and $f_A(t_0) = \pm 1$ into (A.6) gives

$$A = |T/4 - r|, \quad 0 < r < T/2.$$

This value of A is already encompassed in the necessary and sufficient requirements for the existence of a solution (A.5), i.e., it is a boundary case. Consequently we do not determine the full requirements for the existence of this type of solution.

The only other period- T solutions with two switching points that might exist are translations of (A.2) in the dependent variable. Any translation in the dependent variable serves only to increase the value of A required for such a solution to exist.

By substituting (A.3) in to (A.5), we arrive at inequality (7), and this completes the proof. \square

Appendix B. Proof of proposition 2

We now consider the steps given in the proof outline for different parameter values to construct the branches of solutions shown in figure 7.

Appendix B.1. First symmetric branch

We first consider the case, shown in figures 6(a) and 6(b), where a zero in x at $t = t_0 = 1$ coincides with a discontinuity in f_A at $t = t_0 + 1 = 2$, such that

$$\lim_{t \rightarrow (t_0+1)^+} f_A(t) = -A.$$

Figure 6(a)(i) shows the solution after the initial linear segment of solution (step (i) of the construction outline) has been extended by one application of the method of steps. Figure 6(a)(ii) shows the intersections of $x(t - 1)$ and $f_A(t)$; each intersection produces a switching point in the solution shown in figure 6(a)(i).

Figure 6(a)(ii) also shows that (11) holds for this value of t_0 and A . In fact, for the value of t_0 used in figure 6(a)(i) and (a)(ii), the value of A is arbitrary. It remains to find the upper bounds on A such that $x(t) > A$ for $t \in [t_0 + \frac{1}{2}, t_0 + \frac{3}{2}]$.

As the value of A is increased, the number of intersections of $f_A(t)$ and $x(t - 1)$ will also increase; additional switching points are formed in the solution as a result. Figure 6(b)(ii) plots $f_A(t)$ against $x(t - 1)$ for $T/2 < A < T$; figure 6(b)(i) shows the resulting solution with six switching points per period. The symmetries in the forcing ensure that (11) holds independently of the value of A . Thus, a period-4 solution of (1)–(2) will exist provided step (iv), of the construction outline, is satisfied. The periodicity of f_A ensures that as the value of A is increased, assuming (iv) holds, additional switching points emerge in the solution at $A = T/2 + kT$ for $k = 0, 1, 2, \dots$

The minima for $t \in [t_0 + \frac{1}{2}, t_0 + \frac{3}{2}]$ can be calculated from the locations of the intersections of $x(t - 1)$ and $f(t)$. The creation of a general formula for the value of the minima involves enumerating several possible cases, which is a tedious process. However, the existence of the branch can be verified quite easily for $A < \min(T/2, \frac{1}{2})$; for this range of A , there exists only two switching points per period in the solution, at $t = t_0 - 1$ and $t = t_0 + 1$. Consequently, the value of $x(t)$ for $t \in [t_0 + \frac{1}{2}, t_0 + \frac{3}{2}]$ is given by the value of $x(t)$ at the end points of this range, i.e., $x_{\min} = \frac{1}{2}$. Thus, for $T = 4/(1 + 2n)$ where $n = 1, 2, \dots$ there always exists a branch of symmetric period-4 solutions

Appendix B.2. Second symmetric branch

We now consider the case, shown in figures 6(c)(i) and 6(c)(ii), where a zero in x at $t = t_0 = 1$ coincides with a discontinuity in f_A at $t = t_0 + 1 = 2$ such that

$$\lim_{t \rightarrow (t_0+1)^+} f_A(t) = +A.$$

Figure 6(c)(i) shows the solution after the initial linear segment of solution has been extended by one application of the method of steps. Figure 6(c)(ii) shows the intersections of $x(t - 1)$ and $f_A(t)$.

This value of t_0 always produces three intersections of $x(t - 1)$ and $f_A(t)$, creating a dip at the peak of the solution. Similarly to the first branch, equation (11) holds for arbitrary values of A . Additional switching points emerge in the solution at $A = kT$ for $k = 1, 2, \dots$

The minimum value of $x(t)$ for $t \in [t_0 + \frac{1}{2}, t_0 + \frac{3}{2}]$ is located at $t = t_0 + 1$. When there exist only 3 intersections of $f_A(t)$ and $x(t-1)$ per half period (i.e., for $A < \min(T/2, 1/4)$) this minimum is given by $x(t_0 + 1) = 1 - 2A$. Consequently, for $T = 4/(1 + 2n)$ where $n = 1, 2, \dots$ this second branch of symmetric period-4 solutions always exists.

Appendix B.3. Asymmetric branches

When t_0 does not coincide with a discontinuity in f_A as described in the construction of the two branches of symmetric solutions (11) holds only for isolated values of A . These are $A = T/2 + kT$, where $k = 0, 1, 2, \dots$. Figure 6(d)(ii) shows that the intersections of $x(t-1)$ and $f_A(t)$ no longer occur symmetrically about zero. Consequently the solutions are asymmetric, as illustrated by figure 6(d)(i).

When $A = T/2 + kT$, for $k = 0, 1, 2, \dots$, every value of t_0 gives a valid solution. Consequently, the asymmetric branches connect the two symmetric branches for these isolated values of A . When t_0 coincides with a discontinuity, giving a symmetric solution as above, there are two possible ways in which the value of t_0 can change. Either t_0 increases or t_0 decreases. Changing t_0 by a small amount in both directions produces two asymmetric solutions that are symmetric variants of each other, i.e., $x_1(t) = -x_2(-t)$. Thus, two branches bifurcate from each of the symmetric branches and when these solutions branches are plotted, showing $\|x\|$ against A , the branches appear to lie on top of each other. The symmetric solutions are located at the end points of the branch.

For a particular value of A , the conditions for the existence of the asymmetric period-4 solutions are satisfied assuming that the two branches of symmetric solutions exist for the same value of A . \square

References

- [1] Bayer W and an der Heiden U 1998 Oscillation types and bifurcations of a nonlinear second-order differential-difference equation *Journal of Dynamics and Differential Equations* **10** 303–326
- [2] Davis L C 2002 Modification of the optimal velocity traffic model to include delay due to driver reaction time *Physica A* **319** 557–567
- [3] di Bernardo M, Johansson K H and Vasca F 2001 Self-oscillations and sliding in relay feedback systems: symmetry and bifurcations *International Journal of Bifurcation and Chaos* **11** 1121–1140
- [4] di Bernardo M, Kowalczyk P and Nordmark A 2003 Sliding bifurcations: a novel mechanism for the sudden onset of chaos in dry friction oscillators *International Journal of Bifurcation and Chaos* **13** 2935–2948
- [5] Diekmann O, van Gils S, Lunel S M V and Walther H -O 1995 *Delay equations: functional-, complex-, and nonlinear analysis* (Springer)
- [6] Doedel E J, Keller H B and Kernevez J P 1991 Numerical analysis and control of bifurcation problems, part I *International Journal of Bifurcation and Chaos* **1** 493–520
- [7] Doedel E J, Keller H B and Kernevez J P 1991 Numerical analysis and control of bifurcation problems, part II *International Journal of Bifurcation and Chaos* **1** 745–772
- [8] Doole S H and Hogan S J 2000 Non-linear dynamics of the extended Lazer-McKenna bridge oscillation model *Dynamics and Stability of Systems* **15** 43–58

- [9] Engelborghs K, Luzyanina T and Samaey G 2001 *Technical report TW-330: DDE-BIFTOOL v 2 00 a Matlab package for bifurcation analysis of delay differential equations* (Department of Computer Science, K U Leuven, Belgium)
- [10] Fridman E, Fridman L and Shustin E 2000 Steady modes in relay control systems with time delay and periodic disturbances *Journal of Dynamic Systems, Measurement, and Control* **122** 732–737
- [11] Fridman L, Fridman E and Shustin E 2002 *Sliding mode control in engineering* (Marcel Dekker, New York) pp 263–293
- [12] Golubitsky M and Schaeffer D G 1985 *Singularities and groups in bifurcation theory* (Springer-Verlag)
- [13] Hale J K and Huang W 1994 Period doubling in singularly perturbed delay equations *Journal of Differential Equations* **114** 1–23
- [14] Hale J K and Lunel S M V 1993 *Introduction to functional differential equations* (Springer-Verlag)
- [15] Iannelli L, Johansson K H, Jonsson U T and Vasca F 2003 Dither for smoothing relay feedback systems *IEEE Transactions on Circuits and Systems I* **50** 1025–1035
- [16] Kapila V, Haddad W M and Grivas A 1999 Stabilization of linear systems with simultaneous state, actuation, and measurement delays *International Journal of Control* **72** 1619–1629
- [17] Kollár L E, Stépán G and Hogan S J 2000 Backlash in balancing systems using approximate spring characteristics *Periodica Polytechnica Ser Mech Eng* **4** 77–84
- [18] Kollár L E, Stépán G and Turi J 2001 *Proceedings of the fifth Mississippi state conference on differential equations and computational simulations*
- [19] Leine R I and Nijmeijer H 2004 *Dynamics and bifurcations of non-smooth mechanical systems* (Springer)
- [20] Nilsson J, Bernhardsson B and Wittenmark B 1998 Stochastic analysis and control of real-time systems with random time delays *Automatica* **34** 57–64
- [21] Norbury J and Wilson R E 2000 Dynamics of constrained differential delay equations *Journal of Computational and Applied Mathematics* **125** 201–215
- [22] Nordmark A B 1991 Non-periodic motion caused by grazing incidence in an impact oscillator *Journal of Sound and Vibration* **145** 279–297
- [23] Pfeiffer F and Glocker C 1996 *Multibody dynamics with unilateral contacts* (Wiley)
- [24] Richard J -P 2003 Time-delay systems: an overview of some recent advances and open problems *Automatica* **39** 1667–1694
- [25] Ryan E P 1982 *Optimal relay and saturating control system synthesis* (Peter Peregrinus)
- [26] Seydel R 1994 *Practical bifurcation and stability analysis* (Springer-Verlag)
- [27] Sieber J 2004 *Proceedings of 5th IFAC workshop on time-delay systems*
- [28] Stépán G 1989 *Retarded dynamical systems* (Longman)
- [29] Strogatz S H 2000 *Nonlinear dynamics and chaos* (Perseus Publishing)
- [30] Wiercigroch M and de Kraker B 2000 *Applied nonlinear dynamics and chaos of mechanical systems with discontinuities* (World Scientific)
- [31] Zhubsubaliyev Z T and Mosekilde E 2003 *Bifurcations and chaos in piecewise-smooth dynamical systems* (World Scientific)